Electronic Supplementary Material (ESI) for Physical Chemistry Chemical Physics.
This journal is © the Owner Societies 2018

Electronic Supplementary Information

Concentration-dependent photophysical switching in mixed self-assembled monolayers of pentacene and perylenediimide on gold nanoclusters

Daiki Kato,[a] Hayato Sakai,[a] Yasuyuki Araki,[b] Takehiko Wada,[b]
Nikolai V. Tkachenko,*[,c] Taku Hasobe*[,a]

[a]Department of Chemistry, Faculty of Science and Technology, Keio University, Yokohama, Kanagawa 223–8522, Japan

[b]Institute of Multidisciplinary Research for Advanced Materials, Tohoku University, 2–1–1 Katahira, Aoba–ku, Sendai, Miyagi 980–8577, Japan

[c]Laboratory of Chemistry and Bioengineering, Tampere University of Technology, P.O. Box 541, 33101 Tampere, Finland

EXPERIMENTAL

Electrochemical measurements. Cyclic voltammograms were recorded on Iviumstat 20 V / 2.5 A potentiostat by using a three electrode system. A platinum electrode was used as the working electrode. A platinum wire served as the counter electrode, and a saturated calomel electrode was used as the reference electrode. Ferrocene/ferrocenium redox couple was used as an internal standard. All the solutions were purged prior to electrochemical and spectral measurements by using nitrogen gas.

Steady-state spectroscopic measurements. UV/Vis absorption spectra were recorded on Parkin Elmer (Lamda 750) UV-VIS-NIR spectrophotometer. Fluorescence emission spectra were recorded on Parkin Elmer (LS-55) spectrofluorophotometer. Fluorescence lifetimes were also measured on HORIBA Scientific time-correlated single-photon counting system (FluoroCube) with the laser light (DeltaDiode, laser diode head, 404 nm, pulse width: 50 ps and frequency: 1 MHz, respectively) as an excitation source. The practical time resolution is 15 ps by deconvolution of an observed trace with the analytical software (DAS6).

Nanosecond time-resolved measurements. Nanosecond transient absorption measurements were carried out using an Unisoku TSP-2000 flash spectrometer. A Surelite-I Nd-YAG (Continuum, 4–6 ns fwhm) laser with the second harmonic at 532 nm was employed for the flash photo-irradiation exposure to a xenon lamp (150 W) as a probe light and a photomultiplier tube (Hamamatsu R-2949) as a detector. Each sample solution was purged with Ar for at least 20 min prior to the measurement. All experiments were performed at room temperature.

Femtosecond time-resolved transient measurements. Femtosecond transient absorption (fsTA) measurements were carried out using pump-probe setup. Fundamental light pulses at 800 nm wavelength were generated by a Libra F laser system (Coherent Inc.) and the pulse energy was delivered to optical parametric amplifier (OPA) Topas C (Light Conversion Ltd.) to produce the pump pulses at the desired wavelength. For the measurements in the visible region, a Si CCD array was used as a detector. For the measurements in the NIR region, an InGa diode array was used as a detector.

Synthesis

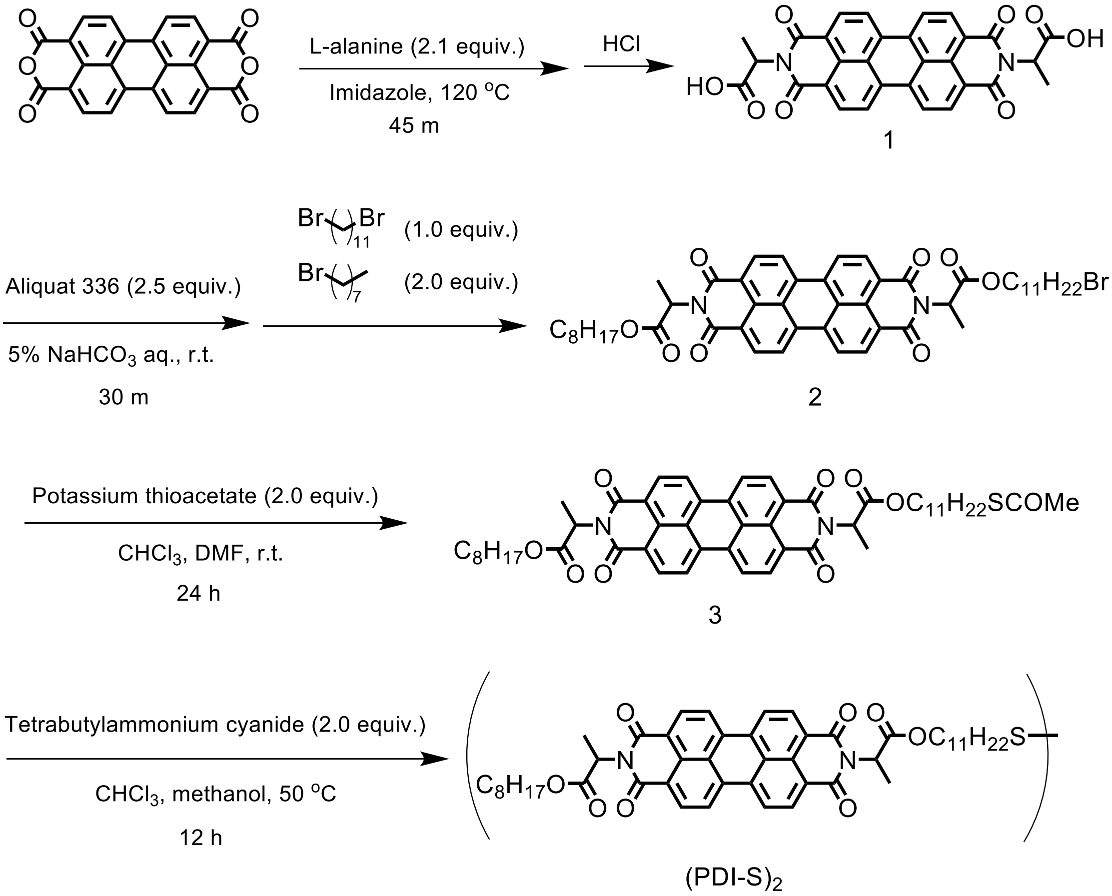

Compound 2: Compound 1 was synthesized by previous reported synthetic route.[1] Aliquat 336 (5.00 g) was dissolved in mixture solution of ethanol/H_2O (1/1, v/v) (50 mL). Next, 5 % $NaHCO_3$ aqueous solution (50 mL) dissolved compound 1[1] (2.67 g, 5.0 mmol) was added to the mixture and stirred stirred at room temperature for 30 m. The synthesized compounds were extracted by $CHCl_3$ and dried over anhydrous $MgSO_4$, and the organic solvent was evaporated. The residue was completely dried at 75 °C for 2 h. Next, the residue was dissolved in dry DMF (30 mL). 1–Bromooctane (1.93 g, 10 mmol) and 1, 11–dibromoundecane (1.57 g, 5 mmol) were added to the mixture stirred at room temperature for 12 h. Then the mixture was poured into 250 mL of methanol. The precipitate was collected by filtration and washed with methanol. After drying the collected compound at 75 °C, the crude was purified by chromatography on silica gel eluting with ethyl acetate/CH_2Cl_2 (1/19, v/v), and compound 2 (yield: 12%, 520 mg, 0.601 mmol) as a red powder was obtained.

^{1}H NMR (400 MHz, $CDCl_3$): δ (ppm): 8.67 (d, J = 7.6 Hz, 4H), 8.58 (m, 4H), 5.78 (q, J = 5.3 Hz, 7.0 Hz, 4H), 4.19 (m, 4H), 3.36, 3.23 (t, J = 7.2 Hz, 6.0 Hz, 2 H), 1.75 (d, J = 6.0 Hz, 6H), 1.60 (m, 6H), 1.21 (m, 24H), 081 (m, 3H); ^{13}C NMR (400 MHz, $CDCl_3$): δ (ppm): 170.27, 162.61, 134.623, 131.65, 129.36, 126.28, 123.13, 65.67, 49.56, 45.14, 34.02, 32.76, 32.55, 31.67, 29.43, 29.12, 28.81, 28.69, 28.44, 28.12, 28.82, 25.89, 22.60, 14.78, 14.03; MS (MALDI–TOF) m/z = 887 [M+Na]

Compound 3: Compound 2 (500 mg, 0.58 mmol) and potassium thioacetate (140 mg, 1.23 mmol) was added to mixture solution of $CHCl_3$/DMF (1/1, v/v) (20 mL) under nitrogen atmosphere and stirred at room temperature for 24 h. After evaporated $CHCl_3$, methanol (50 ml) was added into remaining DMF solution and left the mixture at room temperature for 1 h. The precipitate was collected by filtration. The collected crude was purified by chromatography on silica gel eluting with ethyl acetate/toluene (1/20, v/v), and compound 3 (yield: 48%, 240 mg, 0.279 mmol) as a red powder was obtained.

^{1}H NMR (400 MHz, $CDCl_3$): δ (ppm): 8.41 (d, J = 6.4 Hz, 4H), 8.19 (m, 4H), 5.71 (q, J = 5.2 Hz, 7.2 Hz, 2H), 4.15 (m, 4H), 2.73 (t, J = 7.2 Hz, 6.8 Hz, 2 H), 2.24 (s, 3H), 1.71 (d, J = 6.8 Hz, 2H), 1.42 (m, 24H), 1.17 (m, 3H), 0.74 (m, 3H); MS (MALDI–TOF) m/z = 899 [M+K]

(PDI–S)$_2$: Compound 3 (200 mg, 0.232 mmol) and tetrabutylammonium cyanide (160 mg, 0.596 mmol) were added to mixture solution of $CHCl_3$/methanol (1/1, v/v) (20 mL) under nitrogen atmosphere and stirred at 50 °C for 12 h. After cooling room temperature, (PDI–S)$_2$ was extracted with $CHCl_3$, dried over anhydrous $MgSO_4$ and evaporated. The crude was purified by chromatography on silica gel eluting with ethyl acetate/$CHCl_3$ (1/20, v/v), and (PDI–S)$_2$ (yield: 40%, 76.0 mg, 0.0928 mmol) as a red powder was obtained.

^{1}H NMR (400 MHz, $CDCl_3$): δ (ppm): 8.50 (d, 4H), 8.29 (m, 4H), 5.78 (q, J = 7.0 Hz, 7.2 Hz, 2H), 4.23 (m, 4H), 2.62 (t, J = 7.8 Hz, 8.0 Hz, 2H), 1.78 (d, J = 7.2 Hz, 6H), 1.64 (m, 7 Hz), 1.23 (m, 24 Hz), 0.81 (m, 3 H); ^{13}C NMR (400 MHz, $CDCl_3$): δ (ppm): 170.23, 162.38, 134.23, 131.41, 129.05, 125.80, 122.89, 65.70, 49.62, 39.10, 31.70, 29.42, 29.38, 29.13, 28.46, 25.92, 25.88, 22.62, 14.82, 14.07; MS (MALDI–TOF) m/z = 1689 [M+Cu]

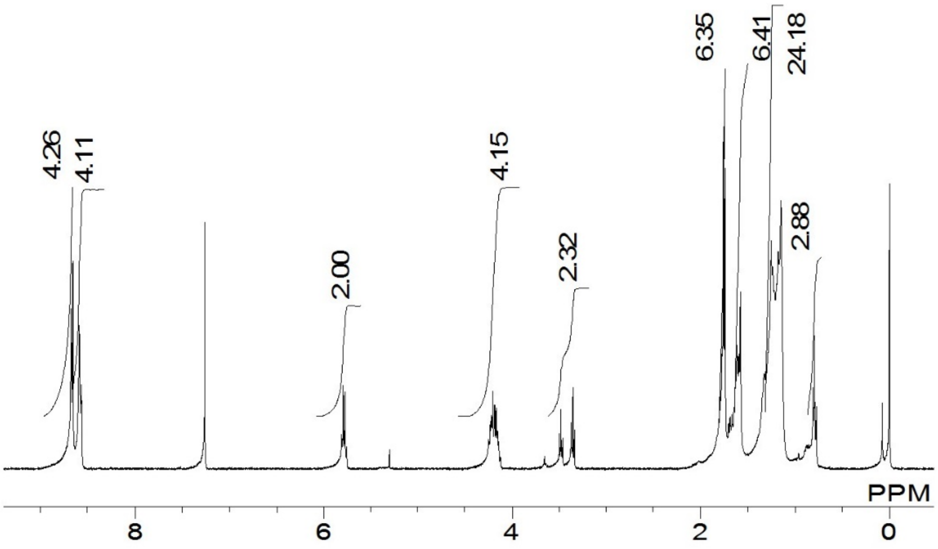

Fig. S1 ^{1}H NMR spectrum of Compound 2.

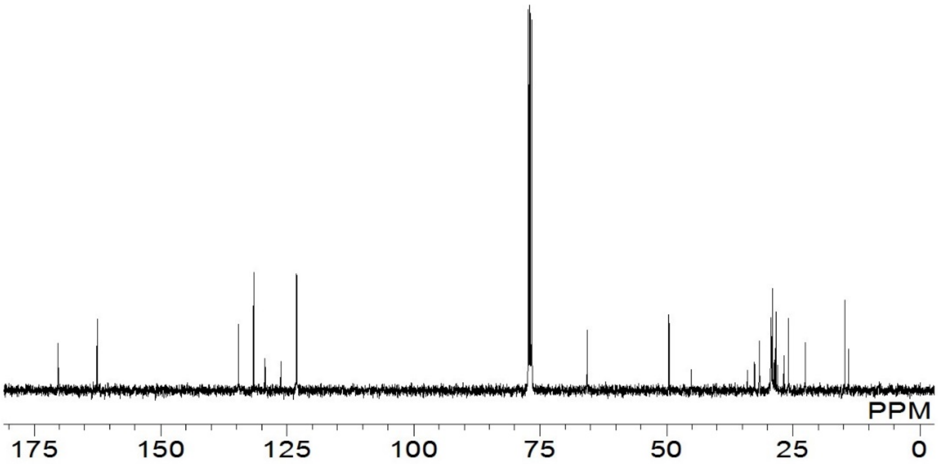

Fig. S2 ^{13}C NMR spectrum of Compound 2.

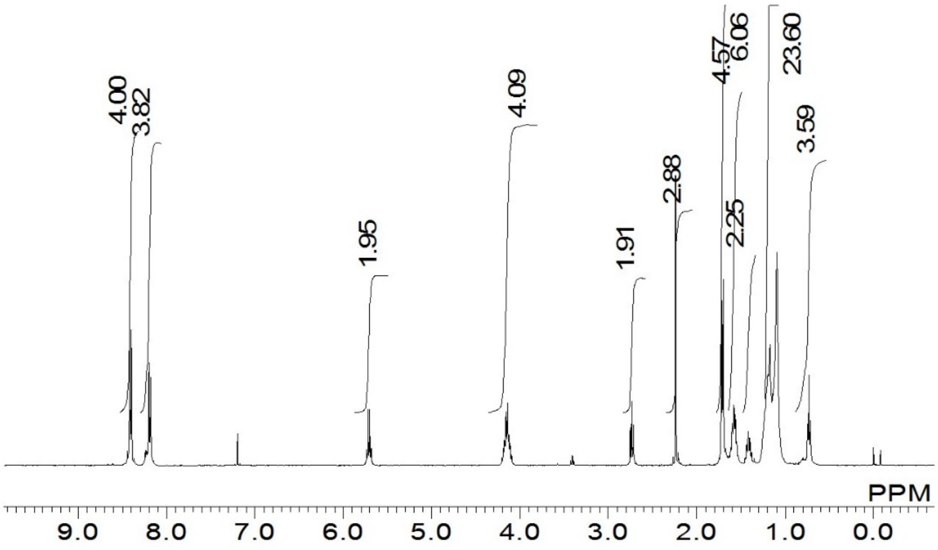

Fig. S3 ^{1}H NMR spectrum of Compound 3.

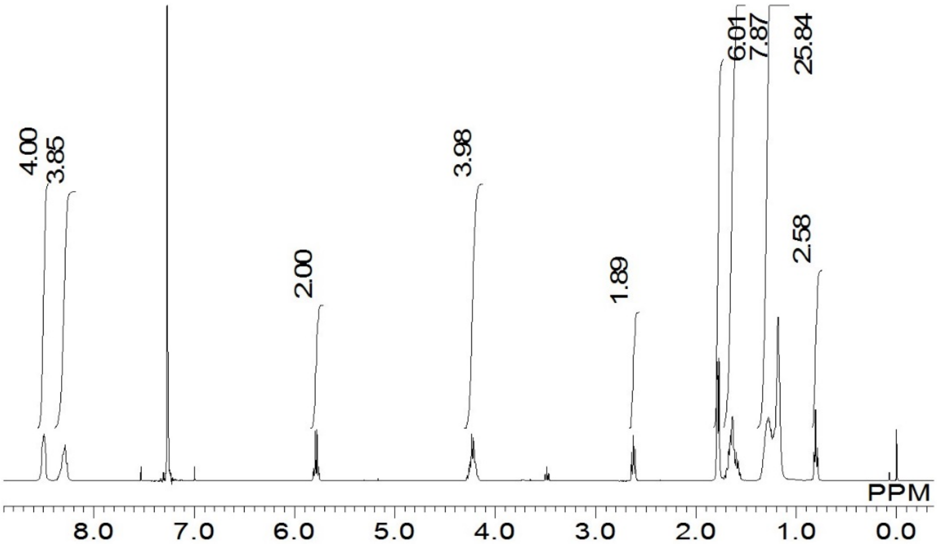

Fig. S4 ^{1}H NMR spectrum of $(PDI–S)_2$.

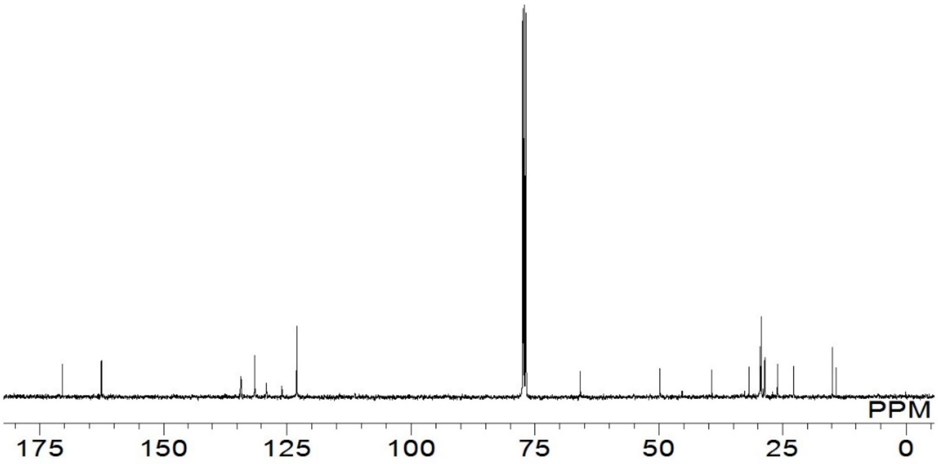

Fig. S5 ^{13}C NMR spectrum of $(PDI–S)_2$.

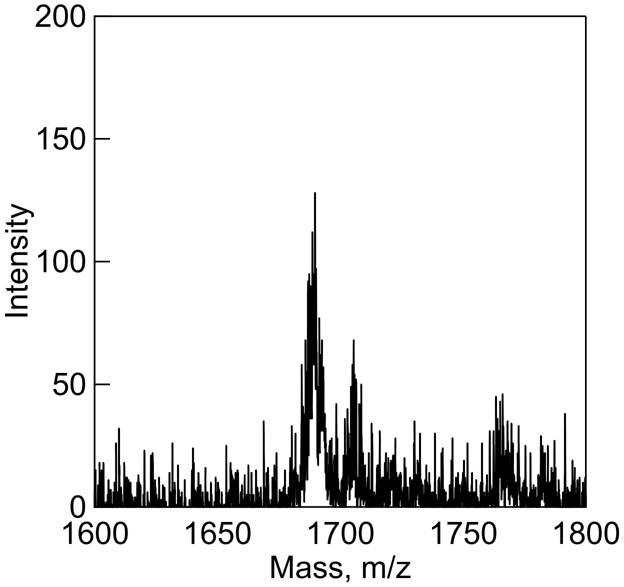

Fig. S6 MALDI–TOF MS spectral profile of (PDI–S)$_2$.

Table S1. Summary of Elemental Analyses of PDI100–GNC and TP*m*–PDI*n*–GNCs.

Compounds		H (%)	C (%)	N (%)	S (%)
PDI100–GNC	Calc.	3.66	38.8	1.85	2.12
	Found	5.83	38.5	0.82	1.43
TP90–PDI10–GNC	Calc.	4.94	45.14	0.10	2.00
	Found	7.30	45.91	0.26	1.24
TP75–PDI25–GNC	Calc.	4.52	42.4	0.46	1.96
	Found	6.64	41.1	0.28	1.23
TP50P–PDI50–GNC	Calc.	4.49	43.8	1.00	2.14
	Found	5.98	43.6	0.90	1.80
TP25–PDI75–GNC	Calc.	4.02	41.2	1.53	2.15
	Found	5.68	40.5	0.61	1.22

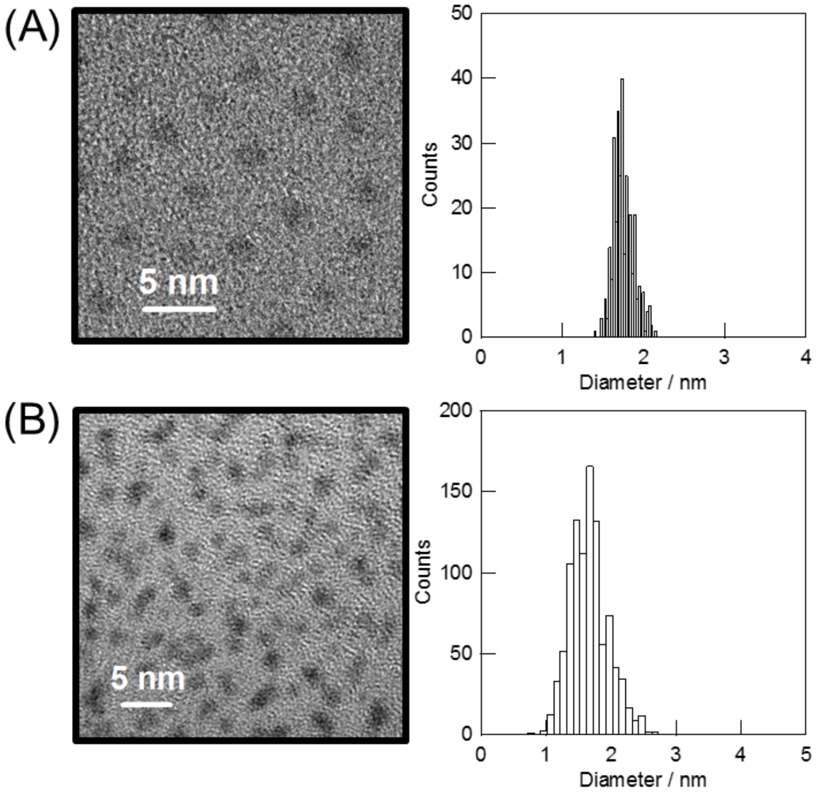

Fig. S7 TEM images and corresponding size distributions of (A) PDI100–GNC and (B) TP100–GNC.

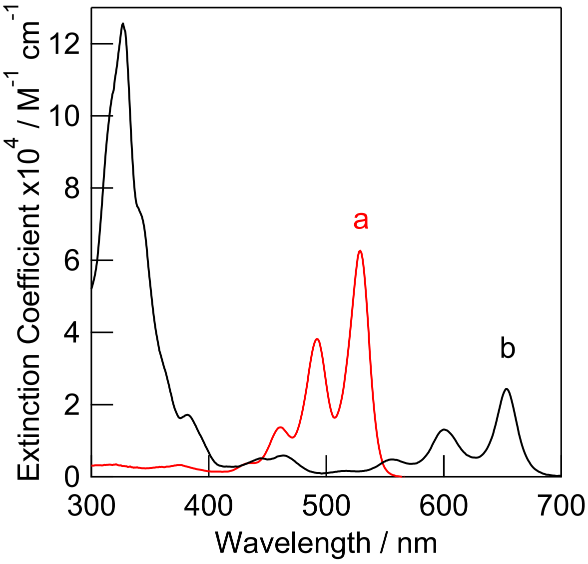

Fig. S8 Absorption spectra of (a) TP–Ref and (b) PDI–Ref in toluene.

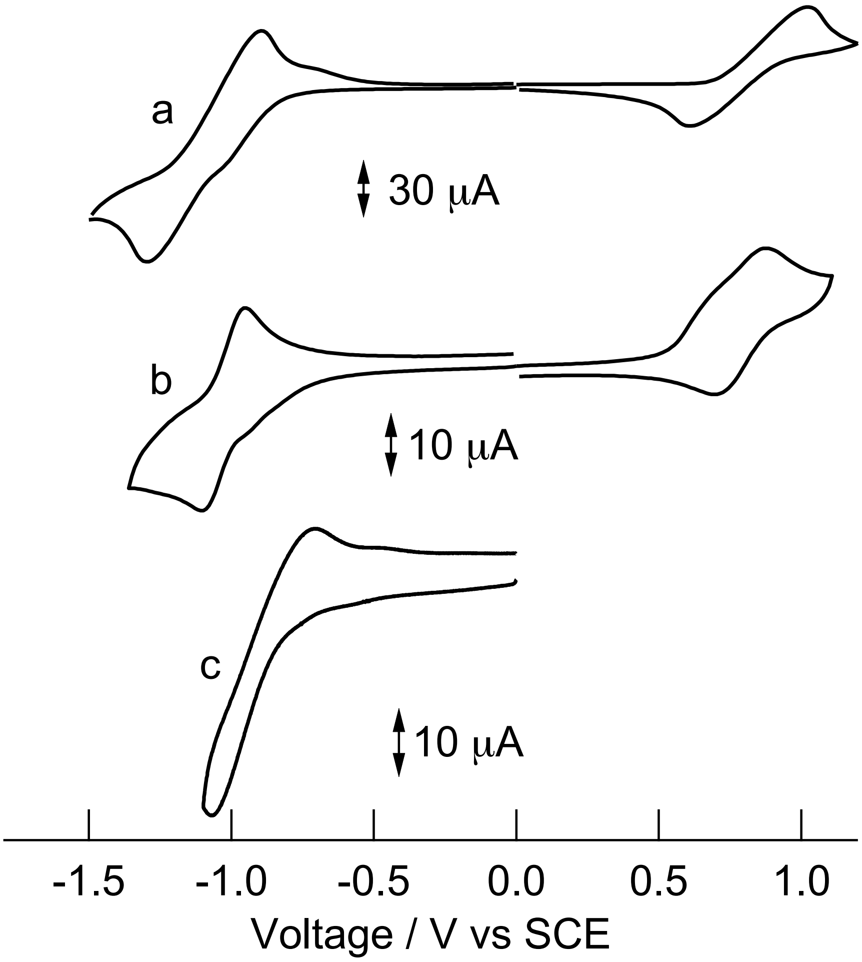

Fig. S9 Cyclic voltammograms of (a) TP-Ref, (b) TP100-GNC and (c) PDI100-GNC in 0.1 M $^{n}Bu_4NPF_6$ in CH_2Cl_2. Scan rate = 100 mV/s, reference electrode: saturated calomel electrode (calibrated to ferrocene).

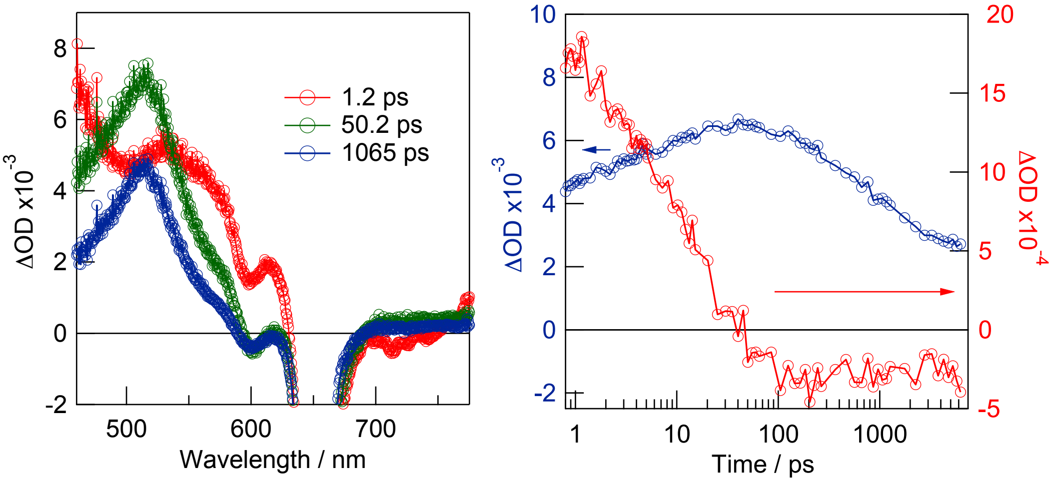

Fig. S10 (Left) Femtosecond transient absorption spectra of TP100–GNC in toluene. (Right) Time profiles at 523 nm (blue line) and at 594 nm (red line). Excitation wavelength is 650 nm.

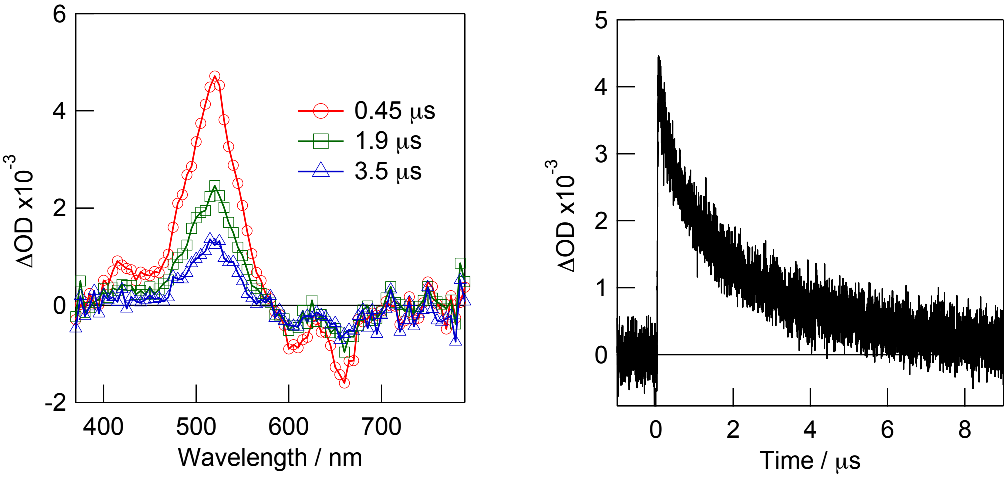

Fig. S11 (Left) Nanosecond transient absorption spectra of TP100–GNC in toluene. Excitation wavelength is 355 nm. (Right) Time profile at 510 nm.

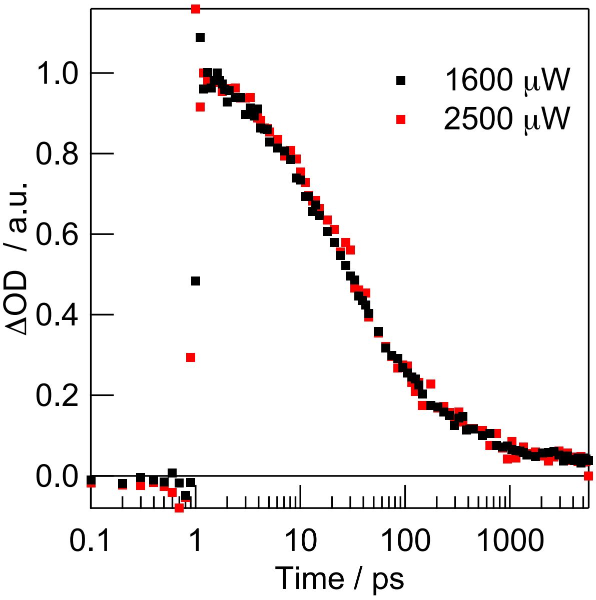

Fig. S12 Normalized time profiles of the femtosecond transient absorption decays of TP90-PDI10-GNC at 590 nm under different laser pulse energy. Excitation wavelength is 650 nm.

Even though we change the laser power intensities, the similar decay curves were observed. Therefore, we can conclude that there is no any sign of the singlet-singlet annihilation and no faster decay at higher excitation. The pentacene absorbance in the samples used for pump-probe experiments was 0.25 at 650 nm. The concentration of excited molecules can be evaluated to be 7.8 $\times 10^{-7}$ M from laser pulse intensity. Therefore, an estimation of the excitation efficiency is 7.8×10^{-7} (M) / 5.2×10^{-5} (M) $\approx$ 1.5%. This means that not more that 1 of 67 pentacene molecules was excited by the pump pulse. According to our estimation an average number of TP molecules attached to one nanoparticle is 49. Thus probability to excite more than one TP on one nanoparticle is < 1%, or negligibly small.

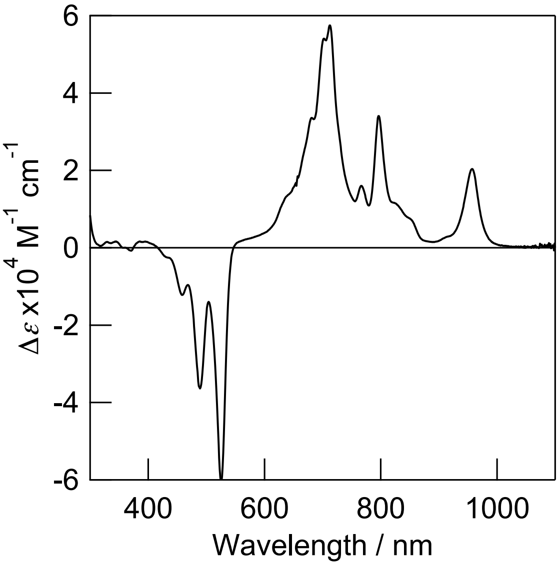

Fig. S13 Differential absorption spectrum (molar extinction coefficient) of $PDI^{\bullet-}$ estimated from absorption spectral changes observed in electron-transfer reduction of PDI-Ref (about 100 μM) by increasing the electrochemical voltages in CH_2Cl_2.

The molar extinction coefficient of $PDI^{\bullet-}$ was calculated using the molar extinction coefficient based on the ground absorption state at 529 nm (62,640 M^{-1} cm^{-1}). The ε ($PDI^{\bullet-}$) at 715 nm was determined to be 57,480 M^{-1} cm^{-1}.

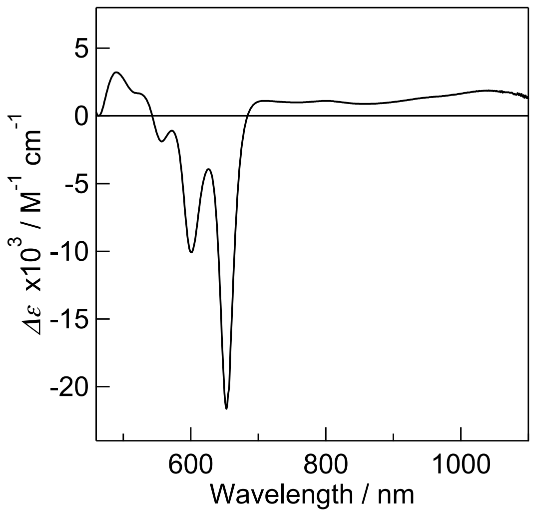

Fig. S14 Differential absorption spectrum (molar extinction coefficient) of $TP^{\bullet+}$ estimated from absorption spectral changes observed in electron-transfer reduction of TP-Ref (about 100 μM) by increasing the electrochemical voltages in CH_2Cl_2.

The molar extinction coefficient of $TP^{\bullet+}$ was calculated using the molar extinction coefficient based on the ground absorption state at at 653 (24,320 M^{-1} cm^{-1}). The ε ($TP^{\bullet+}$) at 715 nm was determined as 1,100 M^{-1} cm^{-1}.

Table S2. Molar extinction coefficients of $TP^{\bullet+}$ and $PDI^{\bullet-}$ at 715 nm and 510 nm. These values are calculated from Figs. S13 and S14.

Species	ε (M^{-1} cm^{-1}) at 715 nm	$\Delta\varepsilon$ (M^{-1} cm^{-1}) at 510 nm
$TP^{\bullet+}$	1,100	1990
$PDI^{\bullet-}$	57,480	–19,510

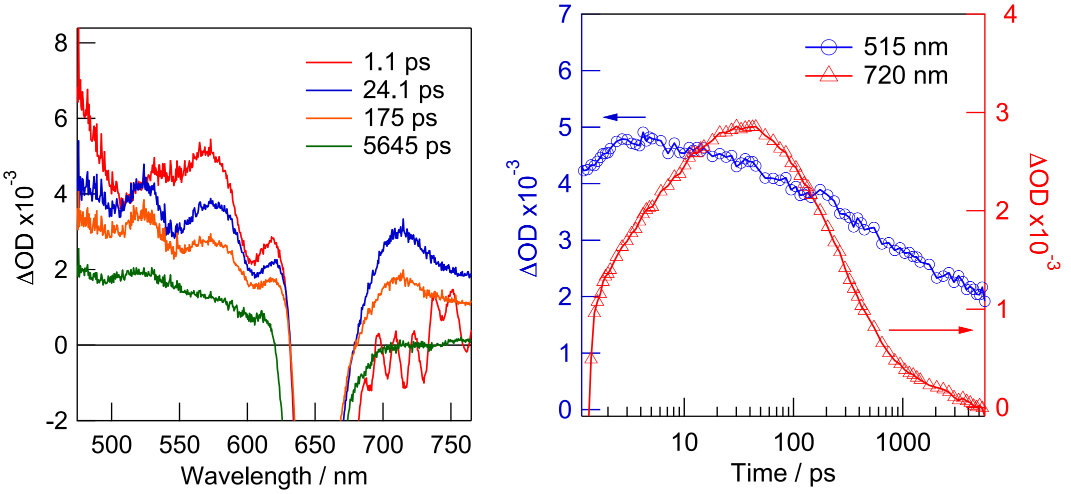

Fig. S15 (Left) Femtosecond transient absorption spectra and (Right) corresponding time profiles of TP75-PDI25-GNC in toluene. Excitation wavelength is 650 nm.

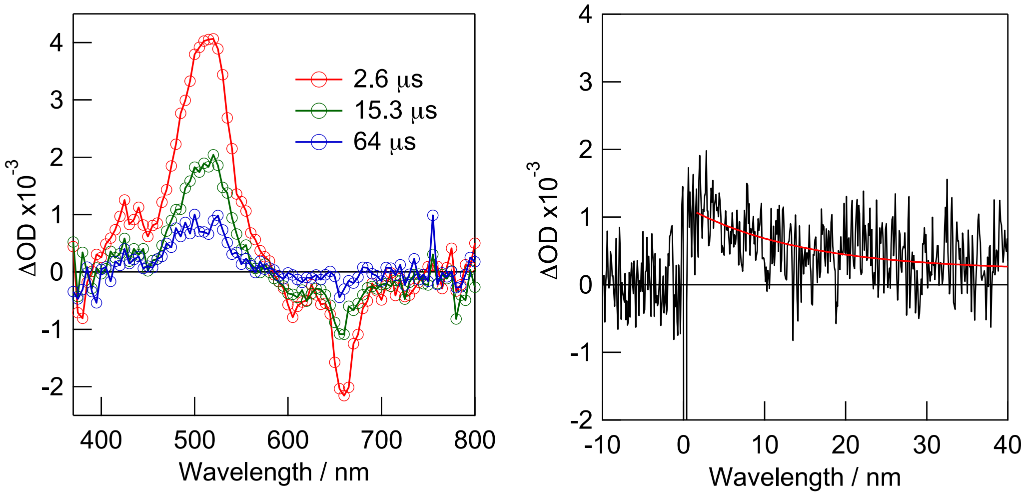

Fig. S16 (Left) Nanosecond transient absorption spectra of TP75-PDI25-GNC in toluene. Excitation wavelength is 355 nm. (Right) Time profile at 510 nm.

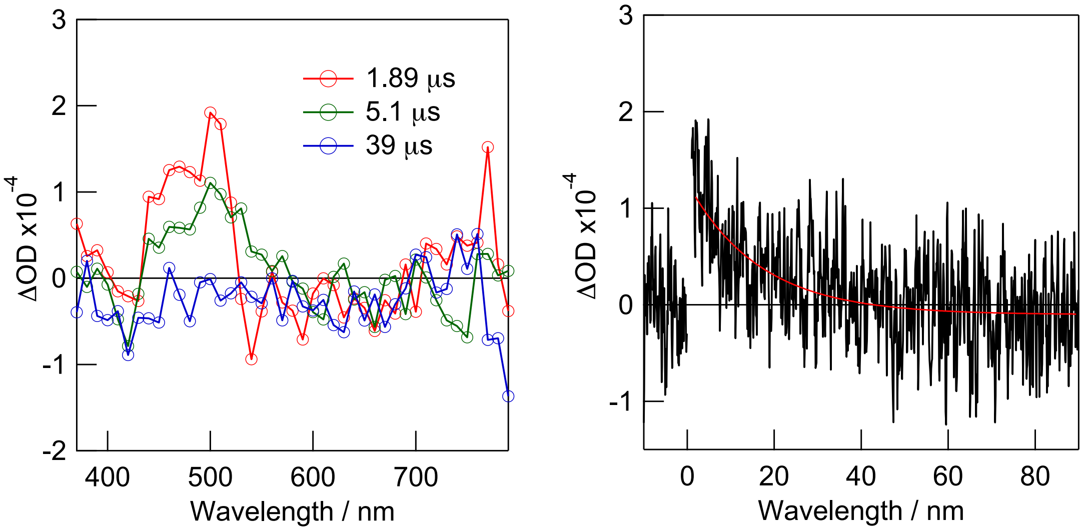

Fig. S17 (Left) Nanosecond transient absorption spectra of TP50-PDI50-GNC in toluene. Excitation wavelength is 355 nm. (Right) Time profile at 510 nm.

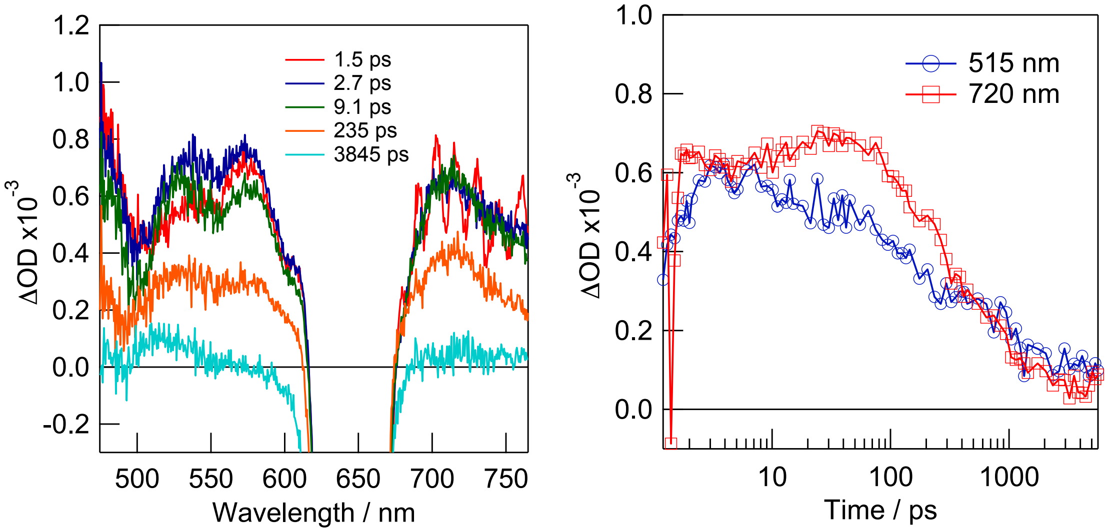

Fig. S18 (Left) Femtosecond transient absorption spectra and (Right) corresponding time profiles of TP25P-DI75-GNC in toluene. Excitation wavelength is 650 nm.

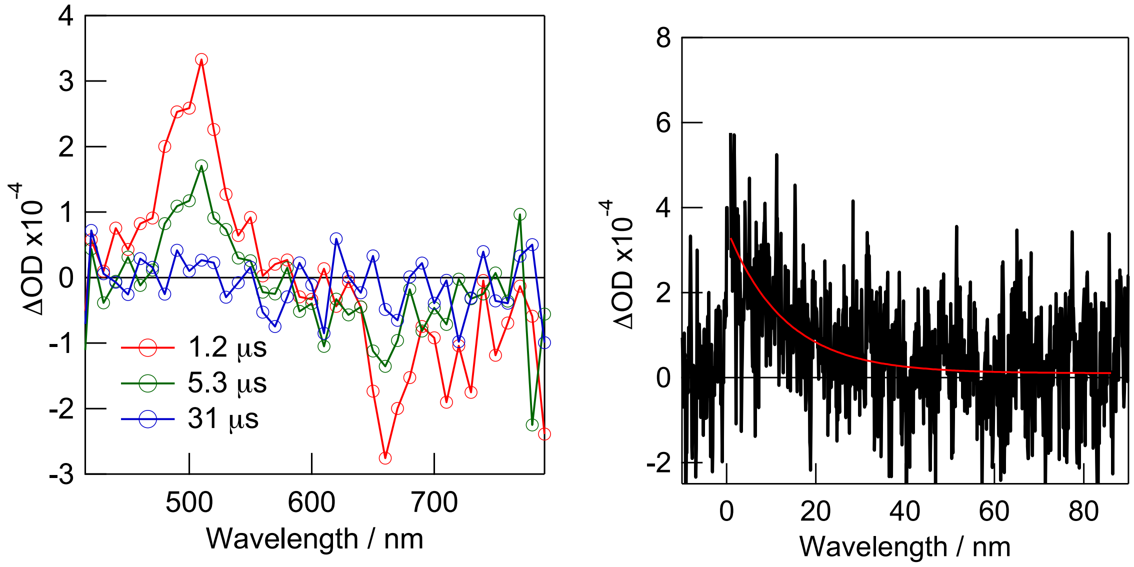

Fig. S19 (Left) Nanosecond transient absorption spectra of TP25-PDI75-GNC in toluene. Excitation wavelength is 355 nm. (Right) Time profile at 510 nm.

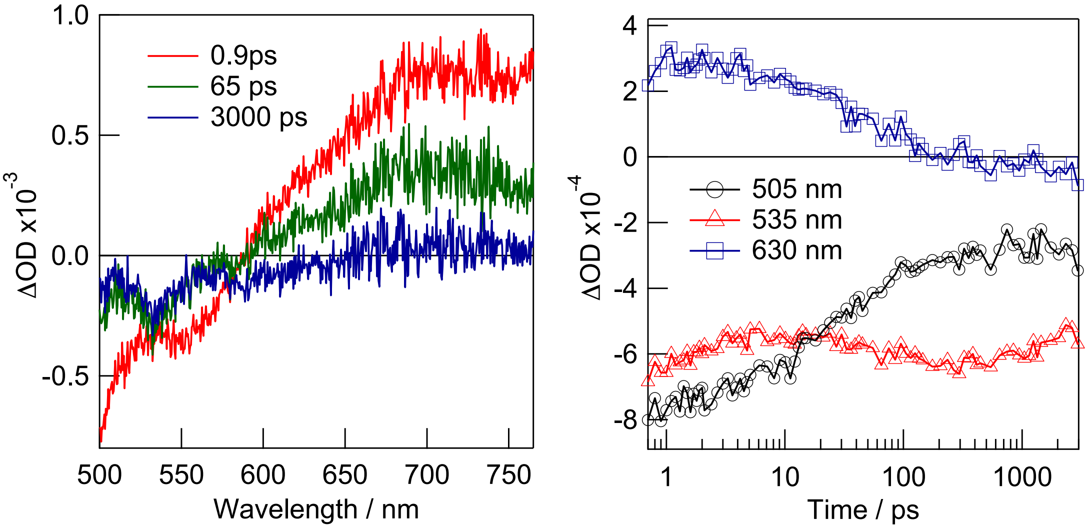

Fig. S20 (Left) Femtosecond transient absorption spectra of PDI100-GNC and (Right) corresponding time profiles in toluene. Excitation wavelength is 480 nm.

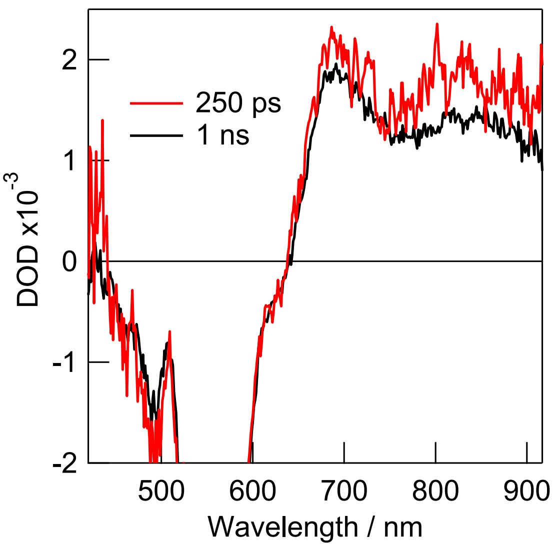

Fig. S21 Picosecond transient absorption spectra of PDI-Mix-GNC in toluene. Excitation wavelength is 532 nm.

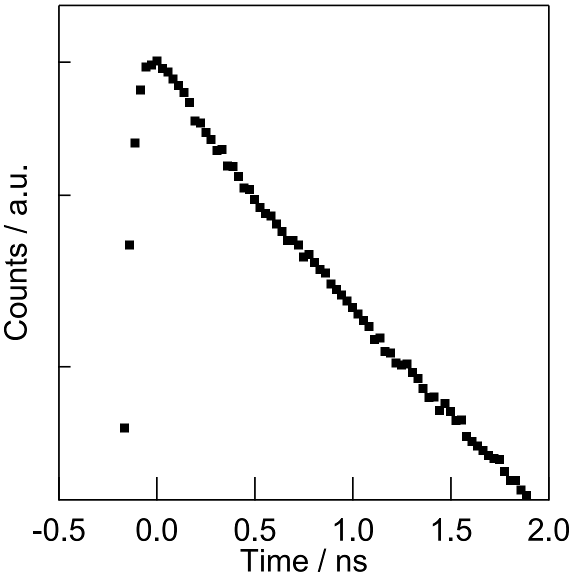

Fig. S22 Time–resolved fluorescence decay profile of PDI-Mix-GNC observed at 600 nm in toluene. Excitation wavelength is 404 nm. The main lifetime analysis: PDI-Mix-GNC: $\tau = 250$ ps.

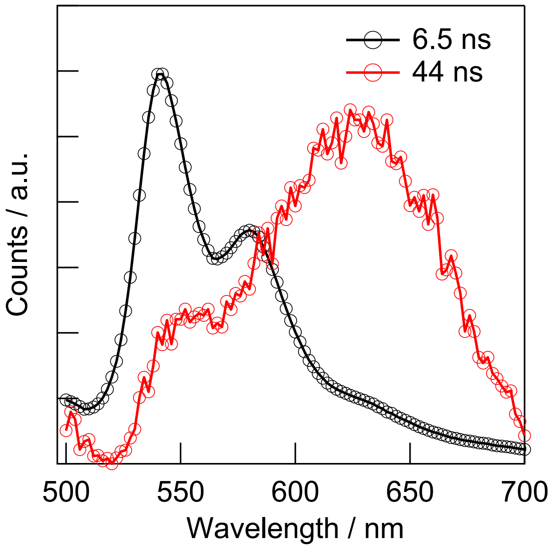

Fig. S23 Time-resolved fluorescence spectra of PDI100-GNC in toluene. Excitation wavelength was 404 nm. The long lifetime spectrum suggested the excimer emission.

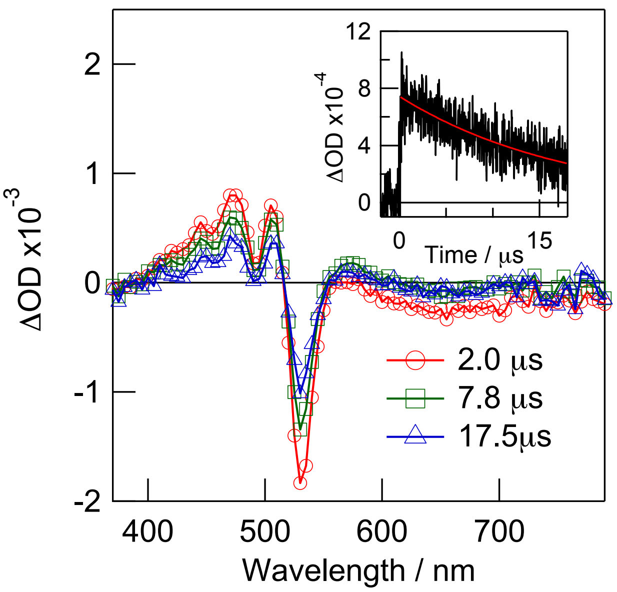

Fig. S24 Nanosecond transient absorption spectra of PDI100-GNC in toluene. Excitation wavelength is 532 nm. The insertion figure shows the time profile of PDI100-GNC at 465 nm (black line) and fitting curve (red line).

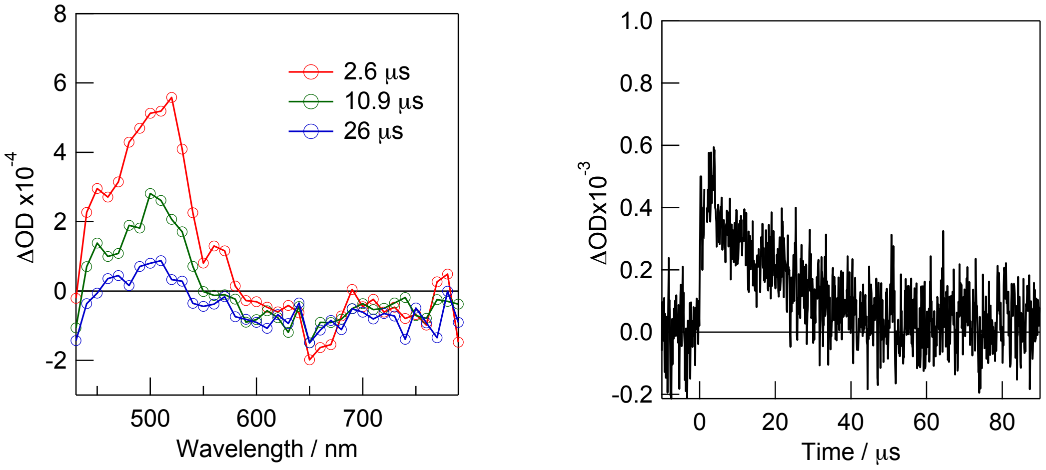

Fig. S25 (Left) Nanosecond transient absorption spectra of TP50-PDI50-GNC in toluene. Excitation wavelength is 532 nm. (Right) Time profile at 510 nm.

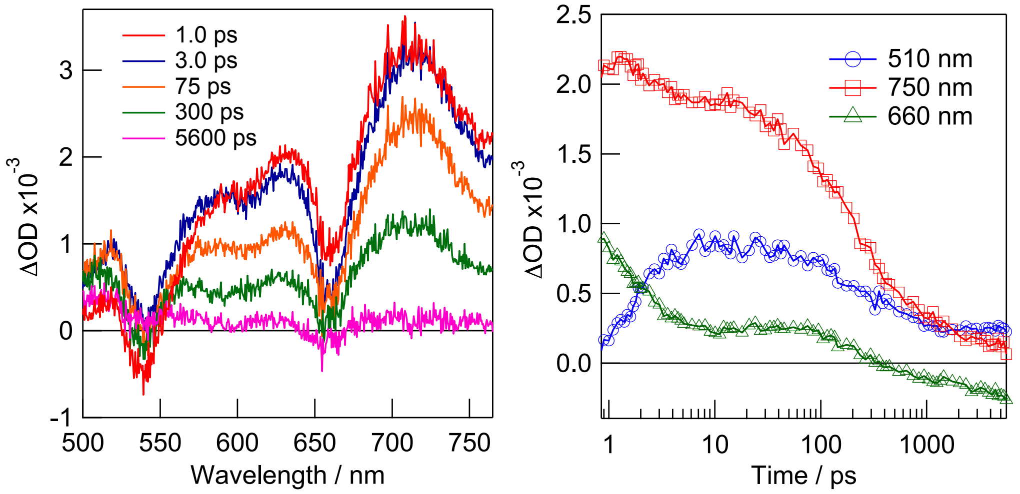

Fig. S26 (Left) Femtosecond transient absorption spectra and (Right) corresponding time profiles of TP75-PDI25-GNC in toluene. Excitation wavelength is 480 nm.

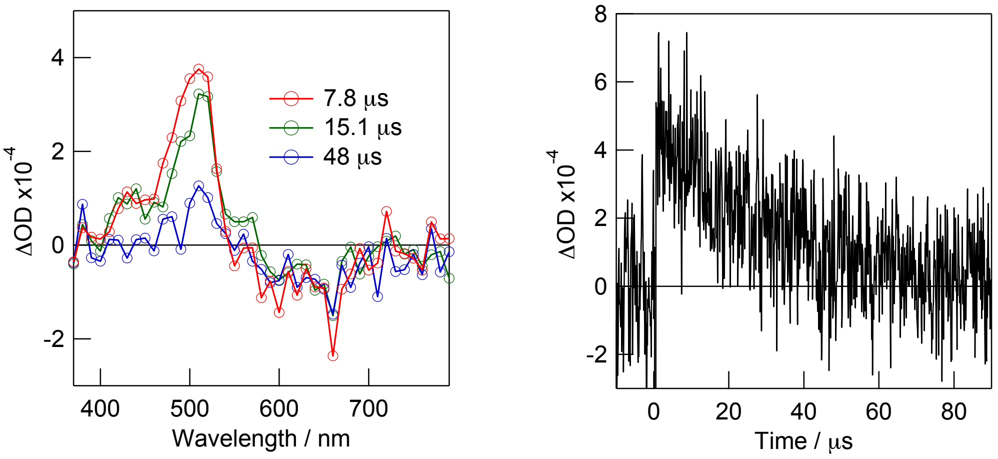

Fig. S27 (Left) Nanosecond transient absorption spectra of TP75-PDI25-GNC in toluene. Excitation wavelength is 532 nm. (Right) Time profile at 510 nm.

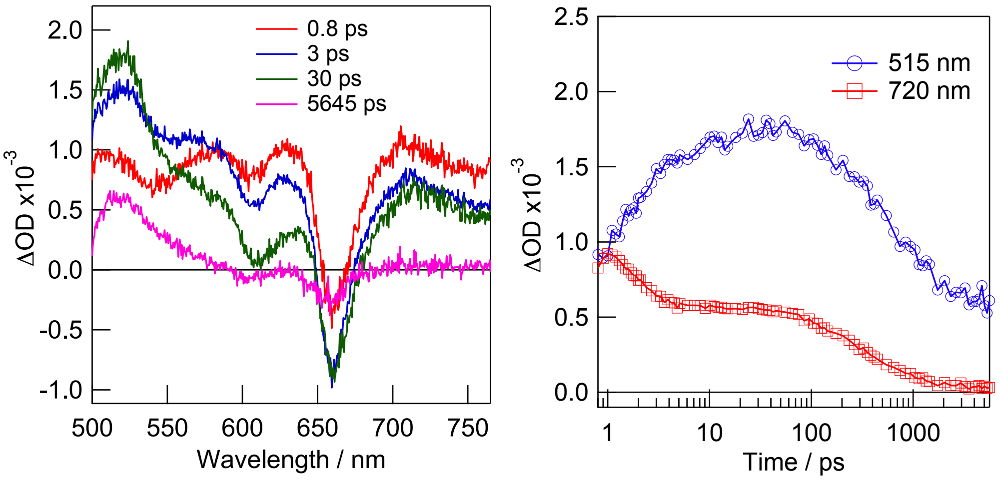

Fig. S28 (Left) Femtosecond transient absorption spectra and (Right) corresponding time profiles of TP90-PDI10-GNC in toluene. Excitation wavelength is 480 nm.

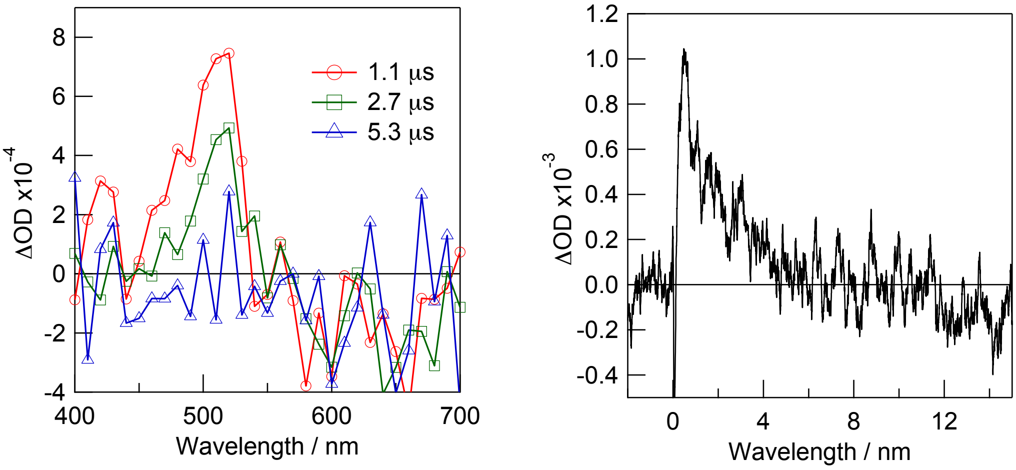

Fig. S29 (Left) Nanosecond transient absorption spectra of TP90-PDI10-GNC in toluene. Excitation wavelength is 532 nm. (Right) Time profile at 510 nm.

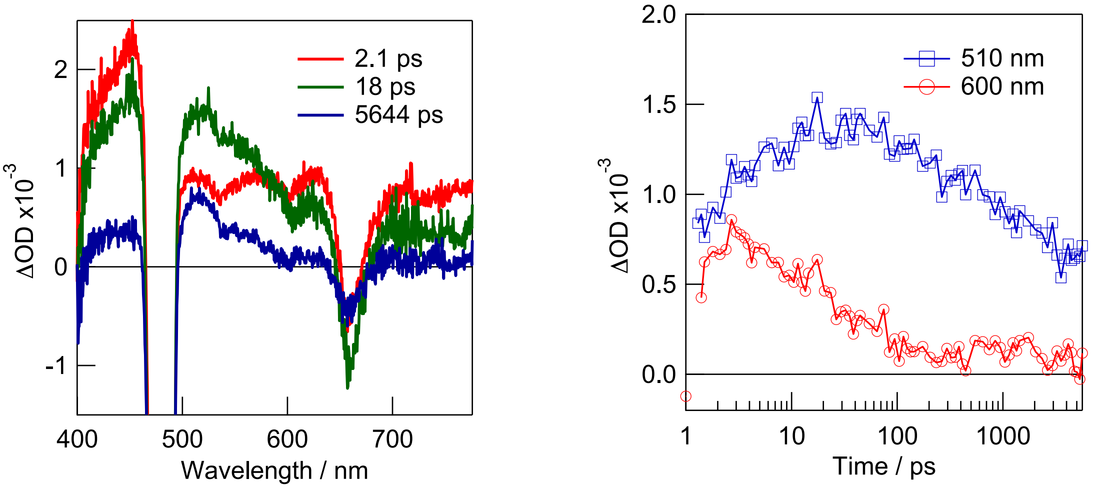

Fig. S30 (Left) Femtosecond transient absorption spectra of TP100-GNC and (Right) corresponding time profiles at 510 and 600 nm in toluene. Excitation wavelength is 480 nm.

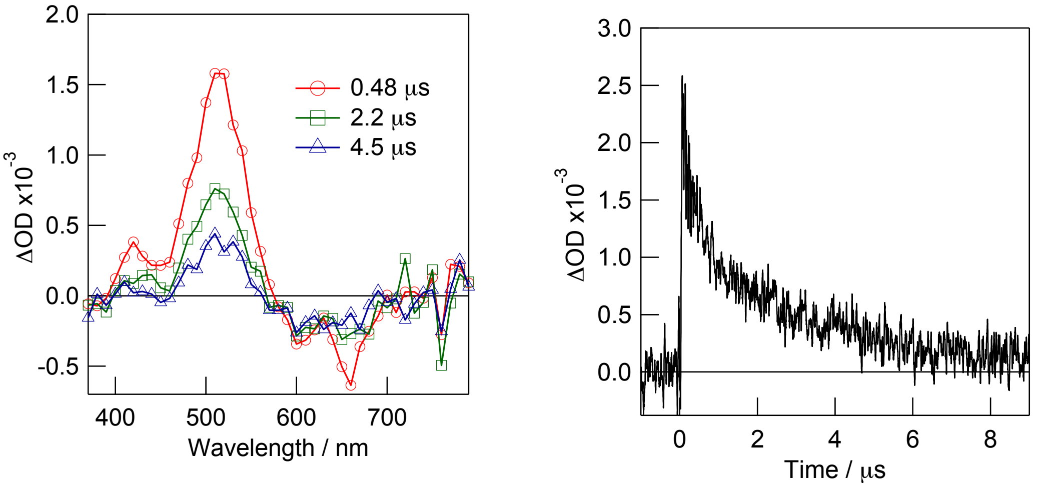

Fig. S31 (Left) Nanosecond transient absorption spectra of TP100-GNC in toluene. Excitation wavelength is 532 nm. (Right) Time profile at 510 nm.

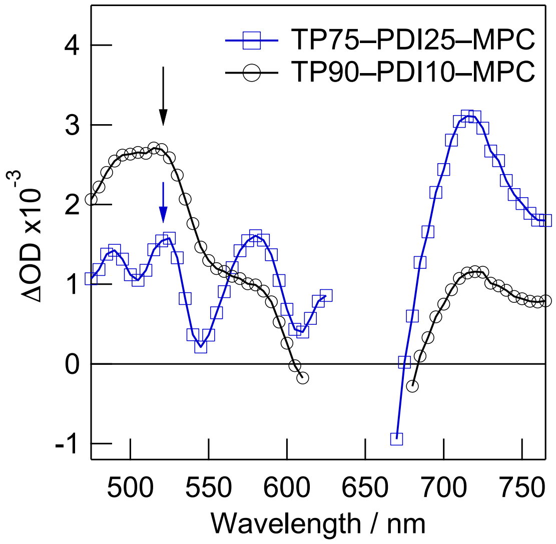

Fig. S32 Decay component spectra at ca. 300 ps lifetime in TP90-PDI10-GNC and TP75-PDI25-GNC (Excitation wavelength: 650 nm). In these cases, we can see the component of ^{3}TP* in the range 500-550 nm in addition to the appearance of electron-transfer product at 715 nm.

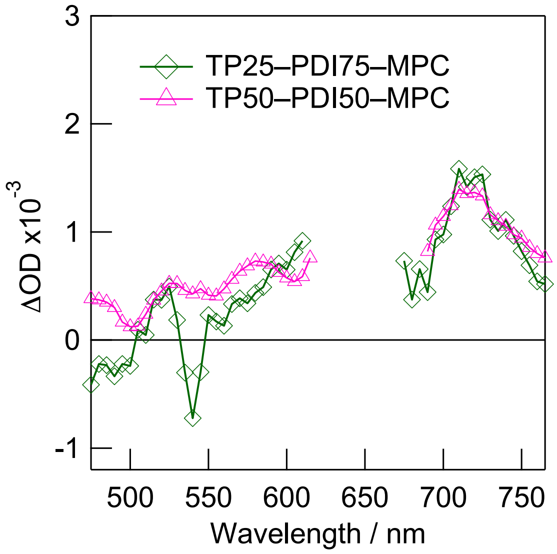

Fig. S33 Decay component spectra at ca. 300 ps lifetime in TP50-PDI50-GNC and TP25-PDI75-GNC (Excitation wavelength: 650 nm). In these cases, the main component is due to the electron-transfer product.

1. Calculation Processes for Electron-Transfer Yields (Φ_{ET}) and Triplet Yields (Φ_{T}) in Case of Excitation at 650 nm

1. 1. Electron-Transfer Yields (Φ_{ET})

The singlet molar extinction coefficient of TP-Ref [$^1\varepsilon$*(TP)] was already reported as 5.97 × 10^4 M^{-1} cm^{-1} at 552 nm.[2] Additionally, the molar extinction coefficient of the charge-separated state ($\mathrm{TP}^{\bullet+}$-$\mathrm{PDI}^{\bullet-}$) [ε($\mathrm{TP}^{\bullet+}$-$\mathrm{PDI}^{\bullet-}$)] was determined to be 58,580 M^{-1} cm^{-1} at 715 nm by adding ε($\mathrm{TP}^{\bullet+}$) and ε ($\mathrm{PDI}^{\bullet-}$) at 715 nm (Table S2).

$^1\varepsilon$*(TP) and ε($\mathrm{TP}^{\bullet+}$-$\mathrm{PDI}^{\bullet-}$) were used to determine the Φ_{ET} of TP*m*-PDI*n*-GNCs. For example, the calculation process in TP90-PDI10-GNC is as follows:

$$\Phi_{\mathrm{ET}}(\text{TP90-PDI10-GNC}) = \frac{\Delta\mathrm{OD}(\mathrm{TP}^{\bullet+}\text{-}\mathrm{PDI}^{\bullet-})\text{at 715 nm} \times {}^1\varepsilon^*(\mathrm{TP})\text{ at 552 nm}}{\Delta\mathrm{OD}({}^1\mathrm{TP}^*)\text{at 552 nm} \times \varepsilon(\mathrm{TP}^{\bullet+}\text{-}\mathrm{PDI}^{\bullet-})\text{ at 715 nm}}$$

$$= \frac{1.16\times10^{-3}\times5.97\times10^{4}\ \mathrm{M}^{-1}\mathrm{cm}^{-1}}{4.58\times10^{-3}\times5.86\times10^{4}\ \mathrm{M}^{-1}\mathrm{cm}^{-1}} = 0.26$$

ΔODs were calculated by curve fittings (exponential fittings). *Δ*OD (singlet) is observed at 1.4 ps from the parent absorption spectra, whereas we used the observed values of ΔOD ($\mathrm{TP}^{\bullet+}$-$\mathrm{PDI}^{\bullet-}$). The Φ_{ET} values were also estimated by the same ways in TP75-PDI25-GNC, TP50-PDI50-GNC and TP25-PDI75-GNC.

1. 2. Triplet Yields of (Φ_{T})

ESI Figs. S32 and S33 show the decay component spectra of TP90-PDI10-GNC, TP75-PDI25-GNC, TP50-PDI50-GNC and TP25-PDI75-GNC, respectively. In TP90-PDI10-GNC and TP75-PDI25-GNC, the mixed components of ^{3}TP* and electron-transfer were observed. In contrast, the main component is due to the electron-transfer products in TP50-PDI50-GNC and TP25-PDI75-GNC. Therefore, we employed the following two different calculation methods as stated below.

1. 2. 1. Triplet Yields (Φ_{T}) of TP50-PDI50-GNC and TP25-PDI75-GNC

The molar extinction coefficient of triplet excited state of TP [$^3\varepsilon$*(TP)] at 510 nm was previously determined to be 5.53 × 10^4 M^{-1} cm^{-1}.[2] ΔODs (triplet) were estimated by curve fittings (Table S3). The calculations for triplet yields (Φ_{T}) were performed by the above-mentioned method of Φ_{ET}.

$$\Phi_{\mathrm{T}}(\text{TP50-PDI50-GNC}) = \frac{\Delta\mathrm{OD}({}^3\mathrm{TP}^*)\text{at 510 nm} \times {}^1\varepsilon^*(\mathrm{TP})\text{ at 552 nm}}{\Delta\mathrm{OD}({}^1\mathrm{TP}^*)\text{at 552 nm} \times \varepsilon({}^3\mathrm{TP}^*)\text{ at 510 nm}}$$

$$= \frac{3.51\times10^{-4}\times5.97\times10^{4}\ \mathrm{M}^{-1}\mathrm{cm}^{-1}}{1.05\times10^{-3}\times5.53\times10^{4}\ \mathrm{M}^{-1}\mathrm{cm}^{-1}} = 0.36$$

1. 2. 2. Triplet Yields (Φ_T) of TP90-PDI10-GNC and TP75-PDI25-GNC

On the other hand, in TP90-PDI10-GNC and TP75-PDI25-GNC, the calculation processes were modified. The ε ($TP^{\bullet+}$-$PDI^{\bullet-}$) at 510 nm was determined as –17,520 M^{-1} cm^{-1}. For example, the calculation process in TP90-PDI10-GNC is as follows:

Time profile at 510 nm was analyzed by tetra-exponential fitting.

$$\Delta OD\ (t) = Y_0 + A_1 \times \exp(-t/\tau_1) + A_2 \times \exp(-t/\tau_2) \\ + A_3 \times \exp(-t/\tau_3) + A_4 \times \exp(-t/\tau_4)$$

These fittings are applied in TP90-PDI10-GNC.

$$\Delta OD\ (t) \text{ at 510 nm} = 0.00153 - 0.0115 \times \exp(-t/1.02\text{ ps}) - 0.00115 \times \exp(-t/8.21\text{ ps}) \\ + 0.00260 \times \exp(-t/418\text{ ps}) + 0.00156 \times \exp(-t/2060\text{ ps})$$

The lifetimes of $^3TP^*$ through SF have multi-lifetime components. Although long-lifetime components (i.e., 418 ps and 2060 ps) were assigned to $^3TP^*$, the lifetime of CS state is ca. 300-400 ps. It is accordingly required to subtract the $\Delta OD(TP^{\bullet+}$-$PDI^{\bullet-})$ from the lifetime component (ca. 300 ps).

$$\therefore \Delta OD(^3TP^*) \text{ at 510 nm} = 0.00153 + 0.00260 + 0.00156$$

$$- \Delta OD(TP^{\bullet+} - PDI^{\bullet-}) \text{at 715 nm} \times \frac{\varepsilon(TP^{\bullet+} - PDI^{\bullet-}) \text{at 510 nm}}{\varepsilon(TP^{\bullet+} - PDI^{\bullet-}) \text{at 715 nm}}$$

$$= 0.00569 - 1.16 \times 10^{-3} \times \frac{-1.75\times10^4\ M^{-1}\ cm^{-1}}{5.86\times10^4\ M^{-1}\ cm^{-1}} = 0.00603$$

Table S3. ΔOD ($TP^{\bullet+}$-$PDI^{\bullet-}$) at 715 nm, ΔOD (singlet) at 552 nm and ΔOD (triplet) at 510 nm in TP*m*-PDI*n*-GNCs.

Compound	ΔOD ($TP^{\bullet+}$-$PDI^{\bullet-}$)	ΔOD (Singlet)	ΔOD (Triplet)
TP90-PDI10-GNC	1.16×10^{-3}	4.58×10^{-3}	6.03×10^{-3}
TP75-PDI25-GNC	3.10×10^{-3}	4.58×10^{-3}	2.98×10^{-3}
TP50-PDI50-GNC	9.10×10^{-4}	1.05×10^{-3}	3.51×10^{-4}
TP25-PDI75-GNC	8.03×10^{-4}	8.55×10^{-4}	3.03×10^{-4}

2. Calculation Processes for Electron-Transfer Yields (Φ_{ET}) and Triplet Yields (Φ_T) in Case of Excitation at 480 nm.

2.1. Electron-Transfer Yields (Φ_{ET})

2.1.1. Electron-Transfer Yields (Φ_{ET}) of TP25-PDI75-GNC and TP50-PDI50-GNC

The molar extinction coefficient of singlet excited state of PDI-Ref [$^{1}\varepsilon$*(PDI)] was calculated to be 3.76×10^{4} M^{-1} cm^{-1} at 755 nm. $^{1}\varepsilon$*(PDI) at 755 nm and ε ($\mathrm{TP}^{\bullet+}$-$\mathrm{PDI}^{\bullet-}$) at 715 nm (see above) were used to determine the Φ_{ET} of TP*m*-PDI*n*-GNCs. As with the above cases of TP excitation, these values were simply calculated by the above method (i.e., ratios of ΔOD (^{1}PDI*) to $^{1}\varepsilon$* (PDI) and ratios of ΔOD ($\mathrm{TP}^{\bullet+}$-$\mathrm{PDI}^{\bullet-}$) to ε ($\mathrm{TP}^{\bullet+}$-$\mathrm{PDI}^{\bullet-}$)) (Table S4).

Table S4. ΔOD ($\mathrm{TP}^{\bullet+}$-$\mathrm{PDI}^{\bullet-}$) at 715 nm and ΔOD (^{1}PDI*) at 755 nm in TP*m*-PDI*n*-GNC.

Compound	ΔOD ($\mathrm{TP}^{\bullet+}$-$\mathrm{PDI}^{\bullet-}$)	ΔOD (^{1}PDI*)
TP25-PDI75-GNC	2.39×10^{-3}	3.53×10^{-3}
TP50-PDI50-GNC	3.34×10^{-3}	4.60×10^{-3}

2.1.2. Electron-Transfer Yields (Φ_{ET}) of TP75-TP25-GNC and TP90-PDI10-GNC

Considering the absorption properties between TP [ε(TP) = 18,720 M^{-1} cm^{-1}] and PDI [ε(PDI) = 2,580 M^{-1} cm^{-1}] at 480 nm, it is impossible to perform selective excitation of PDI in TP90-PDI10-GNC and TP75-PDI25-GNC. Therefore, molecular concentration ratios of TP and PDI should be quantitatively concerned with the calculation processes. For example, the calculation process in TP90-PDI10-GNC following excitation at 480 nm is as follows (see: Table S5 and Table S6):

$$\Phi_{\mathrm{ET}}(\text{TP90-PDI10-GNC}) = \frac{\dfrac{\Delta\mathrm{OD}(\mathrm{TP}^{\bullet+}\text{-}\mathrm{PDI}^{\bullet-})\text{at 715 nm}}{\varepsilon(\mathrm{TP}^{\bullet+}\text{-}\mathrm{PDI}^{\bullet-})\text{ at 715 nm}}}{\dfrac{\Delta\mathrm{OD}(\,^{1}\mathrm{TP}^{*})\text{at 552 nm}}{^{1}\varepsilon*\text{ (TP) at 552 nm}} + \dfrac{\Delta\mathrm{OD}(\,^{1}\mathrm{PDI}^{*})\text{at 755 nm}}{^{1}\varepsilon*\text{ (PDI) at 755 nm}}}$$

$$= \frac{\dfrac{5.70\times10^{-4}}{5.86\times10^{4}\ \mathrm{M}^{-1}\mathrm{cm}^{-1}}}{\dfrac{6.29\times10^{-4}}{5.97\times10^{4}\ \mathrm{M}^{-1}\mathrm{cm}^{-1}} + \dfrac{7.81\times10^{-4}}{3.76\times10^{4}\ \mathrm{M}^{-1}\mathrm{cm}^{-1}}} = 0.31$$

2.2. Triplet Yields (Φ_{T})

2.2.1. Triplet Yields (Φ_{T}) of TP100-GNC

The calculation is performed following our previous report (See: Table S5).[2]

Table S5. ΔOD (^{1}TP*) at 552 nm and ΔOD (^{3}TP*) at 510 nm in TP100-GNC.

Compound	ΔOD (^{1}TP*)	ΔOD (^{3}TP*)
TP100-GNC	9.50×10^{-4}	1.48×10^{-3}

2.2.2. Triplet Yields ($\varPhi_T$) of TP75-TP25-GNC and TP90-PDI10-GNC

As mentioned earlier (section 2. 1. 2.), molecular concentration ratios of TP and PDI should be quantitatively concerned with the calculation processes. For example, the calculation process in TP90-PDI10-GNC following excitation at 480 nm is as follows (see: Table S6 and Table S7):

Time profile at 510 nm was analyzed by tetra-exponential fitting.

$$\begin{gathered}\Delta\mathrm{OD}\ (t) = \mathrm{Y}_0 + \mathrm{A}_1 \times \exp(-t/\tau_1) + \mathrm{A}_2 \times \exp(-t/\tau_2) \\ + \mathrm{A}_3 \times \exp(-t/\tau_3) + \mathrm{A}_4 \times \exp(-t/\tau_4)\end{gathered}$$

This fitting is also used.

$$\begin{gathered}\Delta\mathrm{OD}\ (t) = \mathrm{Y}_0 + \mathrm{A}_1 \times \exp(-t/\tau_1) + \mathrm{A}_2 \times \exp(-t/\tau_2) \\ + \mathrm{A}_3 \times \exp(-t/\tau_3) + \mathrm{A}_4 \times \exp(-t/\tau_4)\end{gathered}$$

$$\begin{aligned}\therefore \Delta\mathrm{OD}(^3\mathrm{TP}^*)\ \text{at 510 nm} &= 0.000537 + 0.000614 + 0.000514 \\ &\quad - \Delta\mathrm{OD}(\mathrm{TP}^{\bullet+} - \mathrm{PDI}^{\bullet-})\text{at 715 nm} \times \frac{\varepsilon(\mathrm{TP}^{\bullet+} - \mathrm{PDI}^{\bullet-})\text{at 510 nm}}{\varepsilon(\mathrm{TP}^{\bullet+} - \mathrm{PDI}^{\bullet-})\text{at 715 nm}} \\ &= 0.00167 - 5.70 \times 10^{-4} \times \frac{-1.75 \times 10^{4}\ \mathrm{M}^{-1}\ \mathrm{cm}^{-1}}{5.86 \times 10^{4}\ \mathrm{M}^{-1}\ \mathrm{cm}^{-1}} = 0.00184\end{aligned}$$

$$\varPhi_\mathrm{T}(\text{TP90-PDI10-GNC}) = \frac{\dfrac{\Delta\mathrm{OD}(\ ^3\mathrm{TP}^*)\text{at 510 nm}}{\varepsilon(\ ^3\mathrm{TP}^*)\ \text{at 510 nm}}}{\dfrac{\Delta\mathrm{OD}(\ ^1\mathrm{TP}^*)\text{at 552 nm}}{^1\varepsilon*\ (\mathrm{TP})\ \text{at 552 nm}} + \dfrac{\Delta\mathrm{OD}(\ ^1\mathrm{PDI}^*)\text{at 755 nm}}{^1\varepsilon*\ (\mathrm{PDI})\ \text{at 755 nm}}}$$

$$= \frac{\dfrac{1.84 \times 10^{-3}}{5.53 \times 10^{4}\ \mathrm{M}^{-1}\mathrm{cm}^{-1}}}{\dfrac{6.29 \times 10^{-4}}{5.97 \times 10^{4}\ \mathrm{M}^{-1}\mathrm{cm}^{-1}} + \dfrac{7.81 \times 10^{-4}}{3.76 \times 10^{4}\ \mathrm{M}^{-1}\mathrm{cm}^{-1}}} = 1.41$$

Table S6. ΔOD ($\mathrm{TP}^{\bullet+}$-$\mathrm{PDI}^{\bullet-}$) at 715 nm and ΔOD ($^3\mathrm{TP}^*$) at 510 nm in TP*m*-PDI*n*-GNC.

Compound	ΔOD ($\mathrm{TP}^{\bullet+}$-$\mathrm{PDI}^{\bullet-}$)	ΔOD ($^3\mathrm{TP}^*$)
TP75-PDI25-GNC	2.94×10^{-3}	9.81×10^{-4}
TP90-PDI10-GNC	3.34×10^{-3}	1.84×10^{-3}

Table S7. ΔOD (^{1}TP* + ^{1}PDI*) in TP*m*-PDI*n*-GNC.

Compound	$\frac{\Delta\text{OD}\,(^{1}\text{TP}^{*})\text{at 552 nm}}{^{1}\varepsilon*\,(\text{TP})\text{ at 552 nm}}+\frac{\Delta\text{OD}\,(^{1}\text{PDI}^{*})\text{at 755 nm}}{^{1}\varepsilon*\,(\text{PDI})\text{ at 755 nm}}$
TP75-PDI25-GNC	2.17×10^{-3}
TP90-PDI10-GNC	1.31×10^{-3}

3. Determination of Kinetics in TP*m*-PDI*n*-GNC.

For example, the calculation process in TP90-PDI10-GNC following excitation of TP units is as follows:

Since the Φ_{ET} can be obtained, the k_{ET} is obtained as follows.

$k_{\text{ET}} = \Phi_{\text{ET}}/\tau_{\text{S1}} = 0.26/20\text{ ps} = 1.3\times10^{10}\text{ s}^{-1}$

Additionally, the lifetimes of singlet excited states of TP or PDI on gold nanoculusters including surface energy transfer to gold surface (k_0) were calculated to be 150 ps and 250 ps by fluorescence lifetimes of TP-Mix-GNC and PDI-Mix-GNC because there is no interaction between neighboring chromophores on gold surface in TP-Mix-GNC and PDI-Mix-GNC.

$$\therefore\ k_0(\text{TP})=\frac{1}{\tau_{\text{S1}}(\text{TP-Mix-GNC})}=\ 6.7\ \times\ 10^{9}\text{ s}^{-1}$$

Finally, the rate constants of singlet fission (k_{SF}) and excimer (k_{EX}) were calculated by substracting k_{ET} and k_0 from the reciprocal of lifetime of singlet-excited states.

$$\begin{aligned}\therefore\ k_{\text{SF}}(\text{TP})&=\frac{1}{\tau_{\text{S1}}(\text{TP90-PDI10-GNC})}-k_{\text{ET}}-k_0\\&=5.0\times\ 10^{10}\text{ s}^{-1}-\ 1.3\ \times\ 10^{10}\text{ s}^{-1}-\ 6.7\ \times\ 10^{9}\text{ s}^{-1}=3.0\ \times\ 10^{10}\text{ s}^{-1}\end{aligned}$$

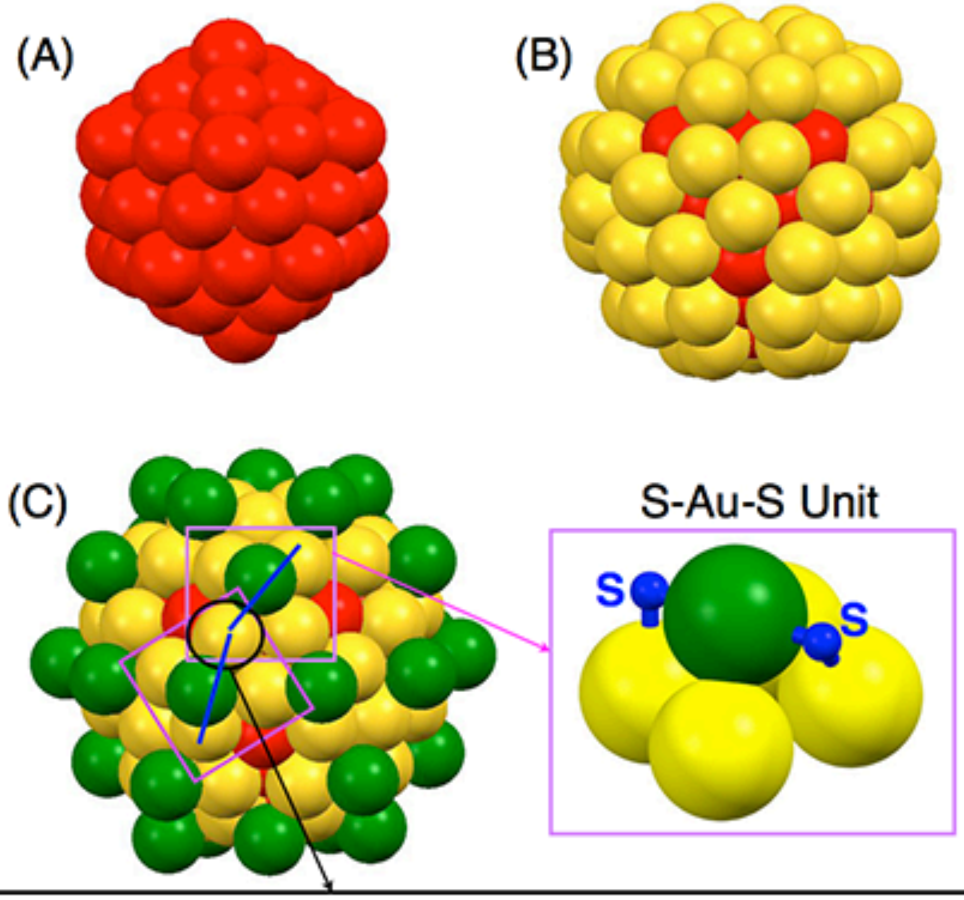

Regarding a certain Au atom (a yellow Au atom with a black circle), there are two possibilities to form a S-Au-S unit (blue line) with neighboring yellow Au atoms.

Fig. S34 A proposed structure of icosahedral $Au_{144}(SR)_{60}$ clusters.[3] (a) gold core consisting of two Mackay icosahedron shells (54 atoms). (b) The icosahedral gold core (red) covered by 60 gold atoms (yellow). (c) The grand core covered in 'staples'. The blue atoms represent sulfur, whereas green atoms represent gold in the staple structure. The organic carbon chains have been left out for clarity. These pictures were prepared using reported materials by H. Häkkinen et al.[3]

The structural alignment of TP and/or PDI derivatives on gold surface can be approximately estimated based on the following hypothesis.

1. The cluster structures such as number of gold atoms and alkanethiol units in TP*m*-PD*n*-GNCs are approximately similar to the above-mentioned icosahedral $Au_{144}(SR)_{60}$ clusters (Fig. S34).
2. According to the reported result,[3] the neighboring Au-Au distances are approximately ~3 Å (ca. 2.8~3.1 Å).

3. In this case (icosahedral $Au_{144}(SR)_{60}$ clusters), 60 gold atoms (yellow atoms in SI Fig. S34) on the icosahedral gold core are available to connect with 60 alkanethiol units. Although the total numbers of molecular units (i.e., sum of number of TP and PDI units in mixed MPCs) on gold surfaces are slightly different in respective systems, we consider the probabilities based on the sum of numbers of TP and PDI units (See: Table 1 in the text).
4. The photophysical processes such as singlet fission, electron transfer and excimer occur by a pair of neighboring dye molecules on gold surface. Therefore, the probabilities of three different molecular pairs (TP-TP, TP-PDI and PDI-PDI) were carefully considered.

A. TP100-GNC

probability of TP-TP pairs: $\frac{{}_{51}P_2}{{}_{51}P_2} = 1$

B. TP90-PD10-GNC

B-1: The probability of TP-TP pairs (for singlet fission) is calculated as follows: $\frac{{}_{49}P_2}{{}_{52}P_2} = 0.89$

B-2: probability of TP-PDI pair: $\frac{{}_{49}P_1 \cdot {}_{3}P_1}{{}_{52}C_2} = 0.11$

B-3: PDI-PDI pair $\frac{{}_{3}P_1 \cdot {}_{2}P_1}{{}_{52}P_2} = 2.26 \times 10^{-3} \approx 0$

C. TP75-PD25-GNC

C-1: probability of TP-TP pairs: $\frac{{}_{33}P_2}{{}_{45}P_2} = 0.53$

C-2: probability of TP-PDI pair: $\frac{{}_{33}P_1 \cdot {}_{12}P_1}{{}_{45}C_2} = 0.40$

C-3: PDI-PDI pair $\frac{{}_{12}P_2}{{}_{45}P_2} = 0.07$

D. TP50-PD50-GNC

D-1: probability of TP-TP pairs: $\frac{{}_{22}P_2}{{}_{47}P_2} = 0.21$

D-2: probability of TP-PDI pair: $\frac{{}_{22}P_1 \cdot {}_{25}P_1}{{}_{47}C_2} = 0.51$

D-3: PDI-PDI pair $\frac{{}_{25}P_2}{{}_{47}P_2} = 0.28$

E. TP25-PDI75-GNC

E-1: probability of TP-TP pairs: $\frac{{}_{8}P_{2}}{{}_{43}P_{2}} = 0.03$

E-2: probability of TP-PDI pair: $\frac{{}_{8}P_{1} \cdot {}_{35}P_{1}}{{}_{43}C_{2}} = 0.31$

E-3: PDI-PDI pair $\frac{{}_{35}P_{2}}{{}_{43}P_{2}} = 0.66$

<u>F. PDI100-GNC</u>

probability of TP-TP pairs: $\frac{{}_{51}P_{2}}{{}_{51}P_{2}} = 1$

References

(1) Xu, Y. J.; Leng, S. W.; Xue, C. M.; Sun, R. K.; Pan, J.; Ford, J.; Jin, S. *Angew. Chem. Int. Ed.* **2007**, *46*, 3896-3899.

(2) Kato, D.; Sakai, H.; Tkachenko, N. V.; Hasobe, T. *Angew. Chem. Int. Ed.* **2016**, *55*, 5230-5234.

(3) Lopez-Acevedo, O.; Akola, J.; Whetten, R. L.; Grönbeck, H.; Häkkinen, H. *J. Phys. Chem. C* **2009**, *113*, 5035-5038.